Local layer structures in circular domains of an achiral bent-core mesogen observed by x-ray microbeam diffraction

Yoichi Takanishi,[1] Toyokazu Ogasawara,[1] Ken Ishikawa,[1] Hideo Takezoe,[1] Junji Watanabe,[1] Yumiko Takahashi,[2] and Atsuo Iida[3]

[1]*Department of Organic and Polymeric Materials, Tokyo Institute of Technology, O-okayama, Meguro-ku, Tokyo 152-8552, Japan*

[2]*Nihon University, Surugadai, Kanda, Chiyodaku, Tokyo 101-8308, Japan*

[3]*Photon Factory, Institute of Materials Structure Science, 1-1 Oho, Tsukuba, Ibaraki 305-0801, Japan*

(Received 3 September 2002; published 21 July 2003)

The local layer structures have been investigated by x-ray microbeam diffraction in the circular domains of the Sm*CP* phase of a banana-shaped molecule. Originally, the molecules form tilted layers with a certain tilt angle as well as nontilted ones. The application of a low electric field induces a tilted layer with a continuous change of the tilt angle; i.e., the tilted layer gradually changes the tilt angle, finally being upright at the center of circular domains. Upon application of a high electric field, the smectic layer forms a cylindrical-type structure. The layer structure changes from cylindrical to onionlike after turning off the high field.

DOI: 10.1103/PhysRevE.68.011706 PACS number(s): 61.30.Gd, 61.10.Eq

I. INTRODUCTION

Since the discovery of the antiferroelectricity in achiral bent-shaped molecules [1,2], extensive studies have been intensively performed. The bent shape provides very interesting and attractive aspects to liquid crystal science from the viewpoint of the relationship between polarity and chirality: Namely, the tilt of achiral bent-shaped molecules induces layer chirality, which may be uniform or alternate from layer to layer, defining the system chirality (overall layer chirality), i.e., homochiral or racemic, respectively [2]. The system chirality and clinicity (synclinic and anticlinic between neighboring layers) specify the polar order, ferroelectric and antiferroelectric; synclinic ferroelectric and anticlinic antiferroelectric structures being homochiral, while synclinic antiferroelectric and anticlinic ferroelectric ones being racemic [3].

The first target compound was P-*n*-(O-)PIMB [1] and their homologous series, in which racemic and homochiral antiferroelectric structures have been identified. Recently, the effects of substituted groups [4–6] and asymmetric end chains [7] on the phase structures have also been discussed. One of the phases of a molecule with asymmetric end chains was suggested to have a homochiral ferroelectric structure. The competition between molecular chirality derived from asymmetric carbons and the layer chirality due to the molecular tilt was also discussed using P-*n*-(O-)PIMB and an analog with asymmetric carbons in the terminal chains [8,9]. The existence of a racemic ferroelectric structure was confirmed by texture observation and second-harmonic generation observations [10].

In determining the molecular orientation of bent-shaped molecules, we always encounter the problem of domain size. Sometimes, application of an electric field is effective to form relatively large domains. However, the field across cells always induces circular domains, though in-plane field is found to be effective in obtaining uniform domains. When one wants to determine molecular orientations or layer chirality in such circular domains based on optical birefringence measurements, information of the local layer structure is also important. In conventional x-ray diffraction measurements, however, only an averaged structure is obtained, because a beam size is at least $0.1\times0.1\ \mathrm{mm}^2$. In this respect, an x-ray microbeam serves as a powerful and effective technique. In this paper, the local layer structures have been investigated by x-ray microbeam diffraction in the circular domains of the Sm*CP* phase of a bent-shaped molecule. It was found that the structures obtained by a different field treatment are quite different, though their textures are optically very similar.

II. EXPERIMENT

The sample used was an achiral banana-shaped molecule, P-10-PIMB, whose chemical structure and phase sequence are shown in Fig. 1(a). Homogeneously aligned cells were prepared using glass plates with indium tin oxide. The glass

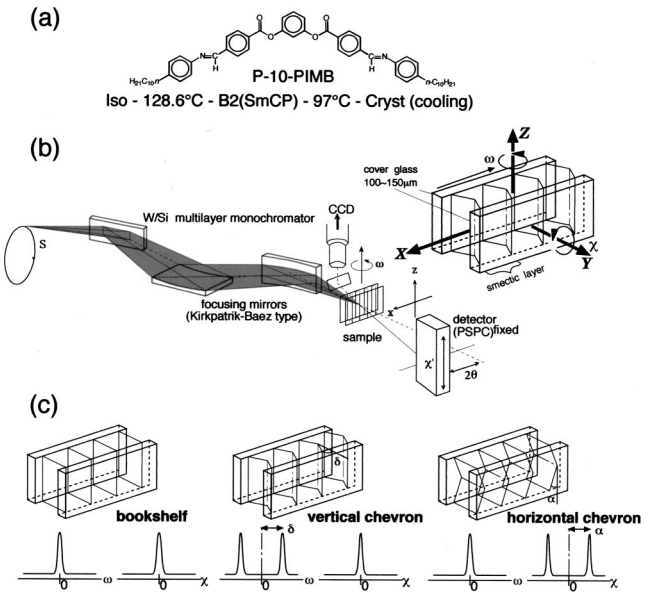

FIG. 1. (a) Chemical structure and phase sequence of a typical banana-shaped molecule. (b) Experimental geometry of the x-ray microbeam diffraction. (c) Schematic illustrations of layer structures and their corresponding ω- and χ-rocking curve profiles.

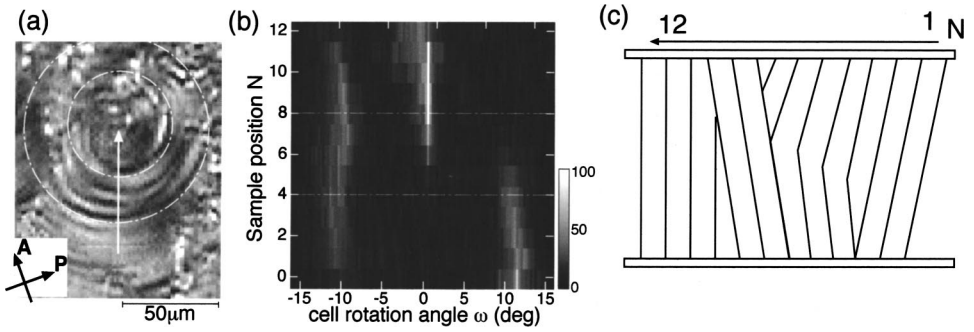

FIG. 2. (a) A photomicrograph of circular domain during application of a very low field. The obtained domain is the coexistence of homochiral and racemic ones. The measurements were made along the white arrow with a step of 5 μm. (b) Two-dimensional (2D) contour plot of ω-scan profiles as a function of irradiated position. Gray scale indicates the diffraction intensity and the ordinate corresponds to the irradiated position step numbers. (c) Spatially varying model layer structure under negligibly weak field.

surface was neither coated with any polymer alignment layer nor rubbed. Sample cell gaps were ca. 8 μm and the thickness of the glass substrates was 150 μm. We could obtain relatively large circular domains by applying an electric field during gradual cooling from the isotropic liquid. In this sample preparation, we used three types of field treatment: (1) 1 kHz, ± 15 V/μm square wave, (2) 5 Hz, ± 3 V/μm triangular wave, and (3) 5 Hz, ± 0.25 V/μm triangular wave. A high square wave [type (1)] induces a racemic domain and a low triangular wave [type (2)] induces a complex structure with racemic and homochiral domains. A very small triangular field [type (3)] was used just to create circular domains without changing the layer structure.

X-ray microbeam measurements were performed at the Photon Factory on the beam line 4*A* (Tsukuba). The x-ray energy was monochromated to 8 keV ($\lambda = 1.55$ Å). The incident beam was collimated using a Si/W multilayer mirror with an angular divergence of 0.5 mrad and the spatial resolution was 3.5×4 μm^2. The detail of the optical geometry is shown in Fig. 1(b) [11,12]. In order to measure the layer tilt angle normal to the substrate, intensity profiles were obtained by rotating a cell about the Z axis (ω scan) normal to the beam with the detector fixed at the 2θ diffraction angle corresponding to the smectic layer spacing. On the other hand, when the layer tilt in the substrate plane was measured, a position sensitive photon counter (PSPC) was vertically located at the 2θ diffraction angle. Since the receiving slit of 2 mm was set just in front of the PSPC, a diffraction peak could be detected even if the layer was tilted in the substrate plane by ca. 30° with respect to the horizontal (X) direction. Thus, the signals detected by the PSPC are equivalent to those obtained by rotating a cell about the cell surface normal (χ scan). Figure 1(c) summarizes schematic profiles expected for bookshelf, vertical chevron (v-chevron) and horizontal chevron (h-chevron) structures [12].

III. EXPERIMENTAL RESULTS

A. Structure during very weak field application

In order to have just a small well-defined domain without deforming the layer structure, a negligibly weak electric field (± 0.25 V/μm) was applied. Figure 2(a) is the texture thus obtained, where homochiral Sm$C_A P_A$ and racemic Sm$C_S P_A$ layers coexist. The x-ray measurements were conducted during application of the field. The ω-scan profiles with a step of 5 μm along the white arrow [see Fig. 2(a)] are shown in Fig. 2(b). At a position far from the circle center ($N = 0$), a sharp single peak was observed at $\omega \sim +12°$, indicating a monotilted layer structure. As the irradiated position approaches the center, another peak appears at $\omega = -11°$ and gradually gains the intensity. Both peak intensities at $\omega = -11°$ and $+12°$ become the same at $N = 4$. This indicates that the layer structure changes from monotilted to chevron. On further approaching the center, the peak at $\omega = +12°$ disappears and the other peak appears at $\omega \sim 0°$. Close to the circle center, the peak at $\omega = 0°$ becomes dominant and the one at $\omega = -11°$ disappears. These results suggest that the layer changes from monotilted to chevron and bookshelf, as illustrated in Fig. 2(c). Instead of the chevron layer structure,

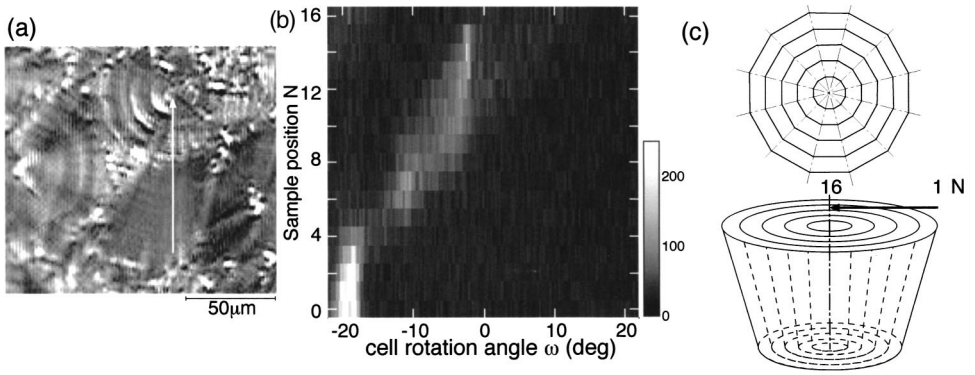

FIG. 3. (a) A photomicrograph of a circular domain during application of a low field. The measurements were made along the white arrow with a step of 5 μm. (b) 2D contour plot of ω-scan profiles as a function of irradiated position. Gray scale indicates the diffraction intensity and the ordinate corresponds to the irradiated position step numbers. (c) Spatially varying model layer structure under a low field.

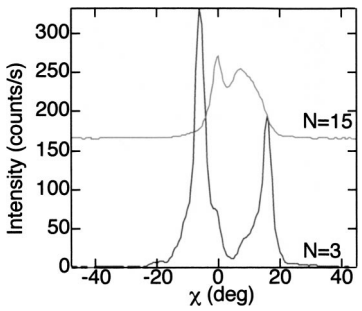

FIG. 4. χ-scan profiles at two irradiated positions ($N=3$ and 15). They were obtained at fixed sample rotation angles, $-20°$ ($N=3$) and $-2.5°$ ($N=15$).

coexistence of opposite monotilted structures is also possible to be postulated even in such a small beam spot. According to the extinction direction of the texture, dotted circles correspond to the boundaries of domains with a different layer chirality [2]. The dotted lines in Fig. 2(b) correspond to the same boundaries, which separate the characteristic three domains dominantly having monotilted, chevron (or oppositely monotilted), and nontilted layer structures.

B. Structure during low field application

To further grow circular domains, a slightly higher voltage wave was applied. Obtained domains were partially circular domains, and the layer chirality was racemic ($\mathrm{Sm}C_SP_A$) and partially mixed domains of opposite homochiral layers as far as we observed the domain textures, as shown in Fig. 3(a). Figure 3(b) shows the ω-scan profile obtained during application of the low field. Data were taken along the white arrow in Fig. 3(a) with 5-μm steps. Apart from the circle center, a sharp single peak is observed at $\omega \sim -20°$, indicating the monotilted layer structure. As the irradiated position approaches the center, the peak becomes broad and its position is gradually shifted to small angles. Finally, in the vicinity of the center, a peak is observed at $\omega=-2°$, indicating almost a nontilted structure. As schematically shown in Fig. 3(c), the spatial variation of the local layer structure is different from that shown in Fig. 2(c). It is interpreted that the applied field smoothens the discontinuous change from the monotilted to the nontilted layer structure.

Now a question arises: How do the molecules arrange in such spatially varying layer structure? Two situations can be imagined in order to compensate for the volume change of each layer due to the spatial variation of the layer tilt angle to the substrate normal, as observed in Fig. 3(b); i.e., (1) in-plane layer tilt (h chevron) is produced or (2) layer thickness spatially changes. To address this problem, two experiments were conducted; χ-scan and layer thickness measurements.

Figure 4 shows the χ-scan profiles observed at $N=3$ and 15, where monotilted and nontilted layer structures are formed, respectively. Contrary to the expectation, the situation is opposite; the monotilted layer region has h-chevron, which cannot compensate for the layer volume change.

The 2θ scan was made to obtain layer spacings at three positions ($N=3$, 8, and 15), where ω peaks were observed at $\omega=-18.4°$, $-11.2°$ (monotilted), and $-2.2°$ (almost nontilted) in Fig. 3(b), respectively. As shown in Fig. 5, only a very small layer spacing difference was observed at three positions. Generally, the layer tilt δ originates from the layer shrinkage due to molecular tilt θ as observed in SmC of rodlike liquid crystalline molecules [13] so that δ varies with temperature dependent θ. If the layer tilt is caused by the layer shrinkage, a layer tilt of 20° corresponds to 6% (2.4 Å) shrinkage of a layer thickness. The present result of almost constant layer thickness indicates that θ does not change in the circular domain. Hence, the only scenario at this stage needed to explain the volume change of each layer associated with the layer tilt is the introduction of wedge dislocations in the layer structure.

Another noticeable observation in Fig. 5 is that the angular distribution of the scattering becomes sharp in the outer region of the circular domain ($N=3$). Together with the fact that the diffraction peak position saturates to about 20° in the outer region [Fig. 3(b)], the tilted layer is concluded to be more favorable. The spatial variation of the layer structure will be discussed later.

C. Structure change by application of a high electric field

It is known that relatively large circular racemic ($\mathrm{Sm}C_SP_A$) domains can be grown by application of a high rectangular wave [14]. Here, we show the layer structures in the presence of such a high field and also after terminating the field. Figures 6(a) and 6(b) show photomicrographs taken during and after the application of a high field. The existence of a relatively large racemic ($\mathrm{Sm}C_SP_A$) circular domain is realized due to the fact that the extinction direction in this domain is parallel to the layer normal during the field application under crossed polarizers, as shown in Fig. 6(a). The appearance of a lot of stripes after turning off the high field [see Fig. 6(b)] is also characteristic to $\mathrm{Sm}C_SP_A$ domains.

The x-ray analysis was made at positions along the white arrows with a 12.5-μm step. The ω-scan profiles during and after the field application are totally different, as shown in Figs. 6(c) and 6(d): Namely, a single sharp peak is observed at $\omega \sim 0°$ at all the irradiated positions [Fig. 6(c)] under the high field, indicating that the layer forms vertical bookshelf

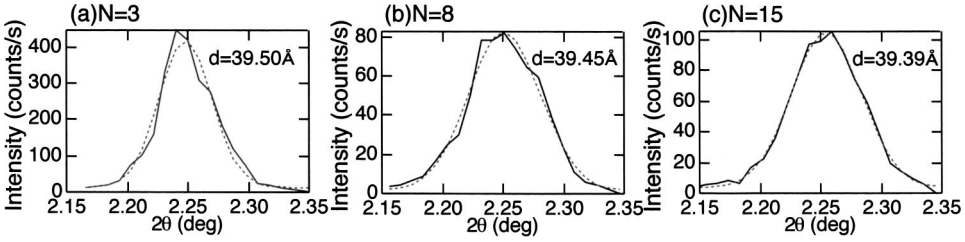

FIG. 5. X-ray diffraction profiles corresponding to the layer thickness at three irradiated positions.

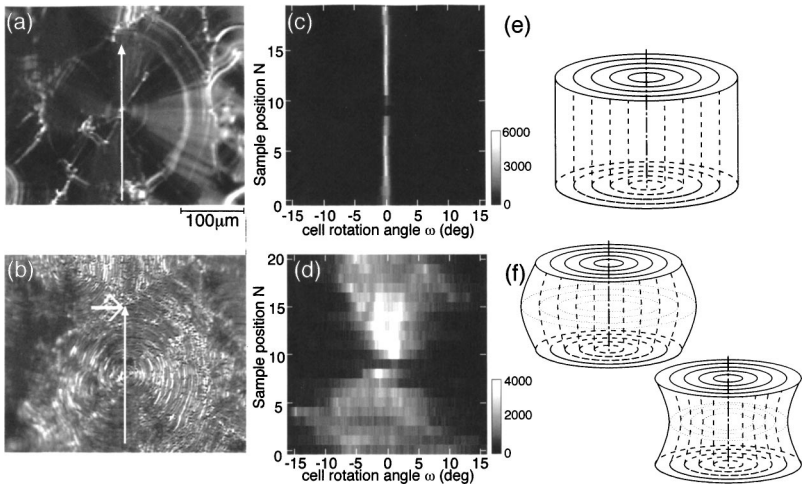

FIG. 6. Photomicrographs of a circular domain (a) during and (b) after the application of a high field. The measurements were made along the white arrow with a step of 12.5 μm. The domain is the same as that in Fig. 3(a). 2D contour plots of ω-scan profiles as a function of irradiated position (c) during and (d) after the application of a high field corresponding to the white arrows in (a) and (b). Gray scale indicates the diffraction intensity and the ordinate corresponds to the irradiated position step numbers. Schematic local layer structures of the circular domain (e) during and (f) after the application of the electric field.

irrespective of the positions in the circular domain. Contrary to the profiles in the presence of a field, the ω-scan profiles after terminating the field strongly depend on the domain position. Apart from the circle center ($N=1$ and 20), a broad peak ranging over more than 10° to both sides of ω is observed, indicating a curved layer structure. As the irradiated position approaches to the circle center, the distribution of the ω-scan peak decreases, and in the vicinity of the center ($N=8-10$), a single peak is observed at $\omega \sim 0°$.

Based on these observations, model layer structures shown in Figs. 6(e) and 6(f), i.e., cylindrical and onionlike (or hand-drum-like) layer structures, are suggested under high and zero fields, respectively. This structure change during and after the field application is quite similar to that observed in the (anti)ferroelectric liquid crystal planar cells of rodlike molecules.

We have also carried out χ-scan measurements under and after applying a high field. The χ-scan profiles under the field change in quite a complicated way with positions, as shown in Fig. 7, where ω was fixed at 0°. This result indicates that the layer is not uniform but has in-plane modulations. The χ profiles at each irradiated position exhibit several peaks and as the irradiated position approaches the circle center ($N=9$), the splitting width of the peak position looks larger. This is because the radius of the circular domain decreases with approaching the center. Most of the observed peaks are not broad, suggesting that the layer is sharply bent in the substrate plane rather than curved.

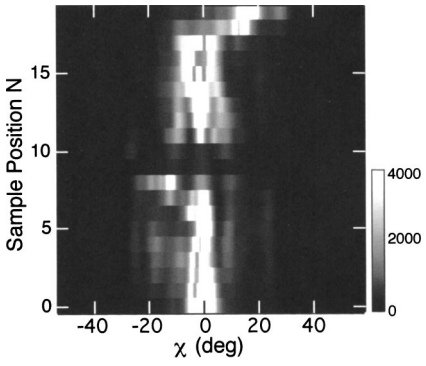

FIG. 7. 2D contour plots of χ-scan profiles as a function of irradiated position during application of a high field. The angle of ω is fixed at 0°.

The situations are different during and after the application of the field. Since the ω-scan profiles have a wide distribution at positions far from the center, the χ-scan profiles for $\omega=-12.8°$, $+0.8°$, and $+10.0°$ are shown in Fig. 8. Apart from the center, a single peak or two peaks can be observed at less than 20° at $\omega=-12.8°$ and $+10°$, and as the position approaches the center, a lot of quite clear peaks are observed at $\omega=0.8°$. Unfortunately, it is hard to give simple model layer structures based on these diffraction data.

IV. DISCUSSION

Let us consider how the layer reconstruction occurs. Assume that the molecules form a bookshelf structure. Two molecular orientations are possible, as shown in Figs. 9(a) and 9(b), where the layer polarizations are (a) parallel and (b) perpendicular to substrate surfaces. Two molecular orientations are also possible for a chevron structure, as shown in Figs. 9(c) and 9(d). Because of the bent shape of the molecule, it is not easy to identify either (a) or (b) or (c) or (d). Actually, there are very few reports that discuss these two kinds of polarization orientations. However, the situation becomes the same when an electric field is applied. Molecules are switched via a rotation on a cone [see (a) and (c)] to realize a ferroelectric order, as illustrated in Fig. 9(e). If the field is strong enough, the polarizations are forced to orient along the field, making the layer upright, as shown in Fig. 9(f). This is a driving force for the chevron-to-bookshelf evolution by a field.

Another problem that we have to discuss is the spatial variation of the layer tilt along the line passing the center of circular domains. As discussed in Sec. III B, tilted layer structures seem to be more stable. This idea is supported by the fact that the layer cannot persist its upright position after terminating a high electric field. Irrespective of chevron or monotilted layer structures, the tilt sense must be opposite at both sides of the center because of the continuity of the layer tilt around the center. Hence, an undefined region may be created at the central part of the circular domain. The simplest solution from the viewpoint of symmetry is an upright

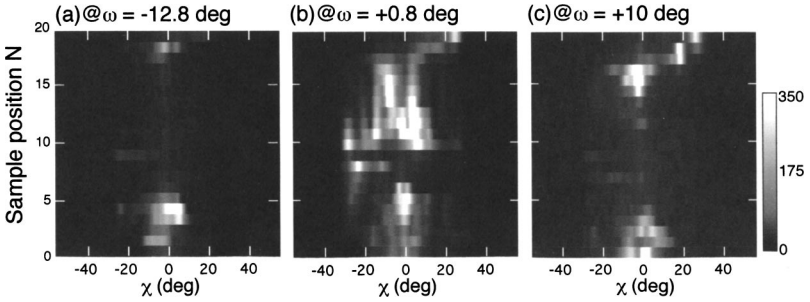

FIG. 8. 2D contour plots of χ-scan profiles as a function of irradiated position after application of a high field. The angle of ω is fixed at (a) $-12.8°$, (b) $0°$, and (c) $+10°$.

orientation. Generally, such kind of spatial variation of layer structures costs a lot of layer deformation energy. However, the layer elasticity in the bent-core mesogen is small, resulting in easily deformable layers. Several experimental facts support this idea: (1) The layer easily changes its structure by application of an electric field of moderate strength, as mentioned in Fig. 6; (2) the spiral texture is frequently observed in the $B7$ phase; and (3) the circular domains always appear in the $B2$ (SmCP) phase. Further experiments and theoretical consideration are necessary to fully understand the nature of the easily deformable layer structure in bent-core mesogen systems.

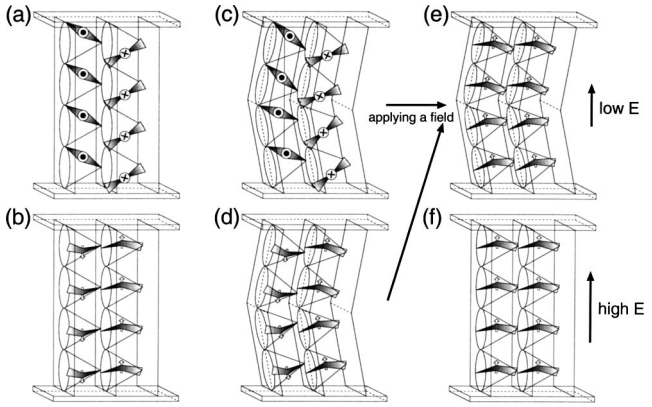

FIG. 9. Schematic illustration of layer structures with different polarization orientations. (a) and (b) bookshelf layer structures, (c) and (d) chevron layer structures. The applied electric field orients polarizations (e) and reconstructs the layer from chevron (e) to bookshelf (f).

V. CONCLUSION

Using x-ray microbeam diffraction, the local layer structures have been investigated in the circular domains of the SmCP phase of a bent-shaped molecule. The layer structure depends on the field treatment, and the smectic layer forms a cylindrical-type structure during the application of a high electric field, while a monotilted layer structure with a spatially varying tilt angle is formed under a low electric field. Moreover, it was found that the layer structures change from cylindrical to onion after turning off the high field. In the case where the applied field was almost zero, the layer structure discontinuously changes, and its boundary corresponds to that of domains with a different layer chirality. No difference of layer thickness was observed at the irradiated positions with different layer tilt angles. All such layer reorientation and spatial variation seem to originate from small layer elasticity of this molecular system.

ACKNOWLEDGMENTS

This work was partly supported by Grant-in-Aid for Scientific Research on Priority Area (B) (Grant No. 12129202) and for an Encouragement of Young Scientists (Grant No. 11750008) from the Ministry of Education, Science, Sports and Culture of Japan. This work was carried out under the approval of the Photon Factory Advisory committee (Grant No. 00G088).

[1] T. Niori, T. Sekine, J. Watanabe, T. Furukawa, and H. Takezoe, J. Mater. Chem. **6**, 1231 (1996).
[2] D. R. Link, G. Natale, R. Shao, J. E. Maclennan, N. A. Clark, E. Korblova, and D. M. Walba, Science **278**, 1924 (1997).
[3] D. M. Walba, E. Korblova, R. Shao, J. E. Maclennan, D. R. Link, M. A. Glaser, and N. A. Clark, Science **288**, 2181 (2000).
[4] G. Pelzl, S. Diele, and W. Weissflog, Adv. Mater. (Weinheim, Ger.) **11**, 707 (1999).
[5] D. Shen, S. Diele, G. Perlzl, I. Wirth, and C. Tschierske, J. Mater. Chem. **9**, 661 (1999).
[6] J. Thisayukuta, Y. Nakayama, and J. Watanabe, Liq. Cryst. **27**, 1129 (2000).
[7] M. Nakata, D. R. Link, F. Araoka, J. Thisayukta, Y. Takanishi, K. Ishikawa, J. Watanabe, and H. Takezoe, Liq. Cryst. **281**, 301 (2001).
[8] M. Nakata, D. R. Link, J. Thisayukta, Y. Takanishi, K. Ishikawa, J. Watanabe, and H. Takezoe, J. Mater. Chem. **11**, 2694 (2001).
[9] J. Thisayukta, J. Watanabe, and H. Takezoe, Jpn. J. Appl. Phys. **40**, 3277 (2001).
[10] F. Araoka, J. Thisayukta, K. Ishikawa, J. Watanabe, and H. Takezoe, Phys. Rev. E **66**, 021705 (2002).
[11] A. Iida, T. Noma, and H. Miyata, Jpn. J. Appl. Phys. **35**, 160 (1996).
[12] Y. Takahashi, A. Iida, Y. Takanishi, T. Ogasawara, K. Ishikawa, and H. Takezoe, Jpn. J. Appl. Phys. **40**, 3294 (2001).
[13] T. P. Rieker, N. A. Clark, G. S. Smith, D. S. Parmer, E. B. Shirota, and C. R. Safinya, Phys. Rev. Lett. **59**, 2658 (1987).
[14] M. Zennyoji, Y. Takanishi, K. Ishikawa, J. Thisayukta, J. Watanabe, and H. Takezoe, J. Mater. Chem. **9**, 2775 (1999).